Colloquia: GCM8

Laser ablation in liquid media of noble metals. The physics of plasma plume and the optical properties of the produced colloids

R. S. Cataliotti(*) and E. Messina

Dipartimento di Scienze Chimiche, Laboratorio di Film Sottili e Nanostrutture
Università di Catania - Viale A.Doria, 6, I-95125, Catania, Italy

Summary. — In experiments of pulsed laser ablation in liquids (PLAL), performed on noble metal targets, many physical aspects regarding the characteristics of the plasma plume generated in the confining liquid, and the optical properties of the produced nanocolloids deserve a clear definition and discussion. In this paper we present the relevant theories and the results of experiments performed in our laboratory on this argument.

PACS 71.35.Cc – Intrinsic properties of excitons; optical absorption spectra.
PACS 43.30.+m – Underwater sound.
PACS 52.35.Dm – Sound waves.

1. – Introduction

In experiments of pulsed laser ablation of solid materials, submerged in liquid environments (PLAL), colloidal suspensions of objects at a nanometer-size scale are obtained. The nature of these nanoparticles and the characteristics of the plasma plume that is surrounding the struck point of the solid target, present a strong dependence on the experimental conditions and deserve a clear description in their physical implications. This because it is possible to modulate the shape and size of the ablated materials, only acting with the pulsed laser beam and regulating its fluence, *i.e.* the amount of energy of the laser electromagnetic field released on the target, expressed in J/cm^2 of surface [1].

In our laboratory, the PLAL technique is commonly carried out with the aim of obtaining nanometer-sized silver and gold particles, which are ideal supports for Surface Enhanced Raman Spectroscopy (SERS) measurements [2]. Such a spectroscopic technique consists in a strong enhancement of the Raman signals, when molecular species are adsorbed on the surface of noble metal colloids.
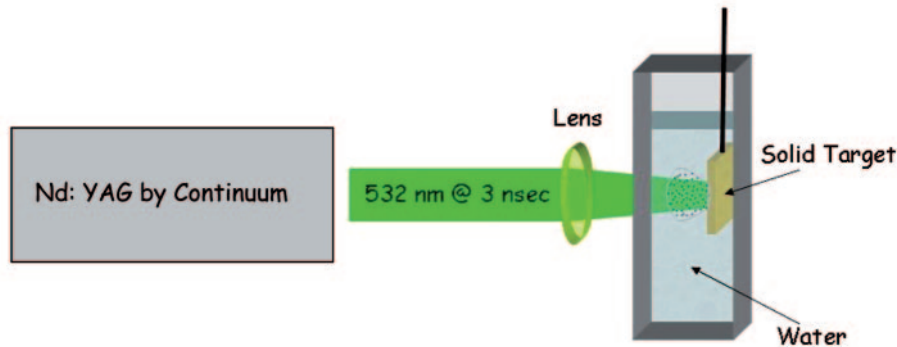
(*) E-mail: rcatalio@unict.it

Fig. 1. – A block scheme of the set-up used in our experiments to produce noble metal nanocolloids in liquid media. Irradiation conditions are described in the text.

It has been ascertained that the signal enhancement is correlated with the optical properties of the metallic nano-object, because their characteristic absorption of visible light enhances the power of electromagnetic field at surface level [3-5].

The purpose of this paper is to describe in details all the physics that underlies these types of experiments that we are engaged in. In particular, we will treat the characteristics of the plasma plume as a system that is out of the thermodynamic equilibrium, and in which sound waves propagate under the confining action of the liquid medium. We will present the optical properties of the noble metal nanoparticles, their dependence on size and shape, and the theories more used to explain these properties.

Therefore, after the experimental section, the paper is divided into two parts. In the first one, the characteristics of the plasma plume are treated. In the second one, the theories that explain the plasmonic resonances (PR) and their dependence on the optical properties of these nanostructured colloidal particles are discussed.

2. – Experimental section

In fig. 1 the simple set-up we used to perform PLAL experiments is shown. Briefly, it consists of a pulsed laser source, which is a Nd:YAG by *Continuum*, model *Surelite II*, operating at 532 nm in the second harmonics. The laser beam has been focused on the target by a lens of 250 mm focal length and the target was submerged in the liquid medium that in our case has been water. Typical irradiation conditions have been: pulses repetition was set at 10 Hz with 3 ns pulse duration; the irradiation period has been protracted for twenty min. The laser spot size on the surface has been varied in the range 1–3 mm of diameter to get always an energy density on the target (fluence) of around 400 mJ/cm^2. It was observed that, when we varied the asset of experiments by suspending vertically the target in the liquid medium, instead to put it in the vessel bottom, and irradiate sending the laser beam at 90 degrees to the sample, a clear double layer having particles suspended on the top was observed in the irradiated zone only. This phenomenon was more clearly visible with gold than with silver, due to intense red colour of gold colloids. Suspending the irradiation and allowing the system to restore equilibrium conditions, diffusion of Brownian particles in the whole submerging fluid was observed in a few minutes [6]. During irradiation a typical plasma plume was observed

Fig. 2. – A 1000 times magnification of the plasma plume generated in water by pulsed laser ablation of solid noble metal targets.

and its appearance is that shown in fig. 2. The strong luminosity is due to electromagnetic radiation emission by the ionic states of metal atoms in the plasma. At the end of irradiation, we observed a coloured colloidal suspension of gold or silver in water, that appeared red or yellow, respectively. The aqueous suspension was transparent and just ready for optical measurements in the visible spectral region.

Analysis of the plasma plume was performed observing the propagation of sound waves in the liquid confined region around the struck point, whereas the shock waves in the solid target were studied at the light of Courant [7] and Cole [8] treatments, that consider the failure of the Navier-Stokes equations to treat this matter. The colloidal suspensions of noble metal particles were subjected to spectral analysis using a Perkin Elmer Lambda 2 spectrometer in the region 300–1100 nm, with a 1 nm resolution power. The extinction of each sample was monitored in the relevant plasmonic resonance (PR) region that is around 400 nm for silver and around 530 nm for gold [9]. Typical PR spectra of these samples are shown in fig. 3. The reader may see the noticeable intensity difference between gold and silver PR spectra [9]. The role played by the complex dielectric constant of the two metals in producing these differences has been analysed.

3. – Results and discussion

3`1. *The physics of processes involved in the plasma plume*. – When a laser ablation experiment is carried out in a liquid medium, the confinement action operated by the liquid in which the ablated solid target is submerged determines the formation of a shock wave in the plasma plume [10-12]. The laser produced plasma tends to expand at a supersonic velocity, but this expansion creates the shock waves because the liquid confines the expansion itself. The laser energy of pulses, impinging on the solid target,
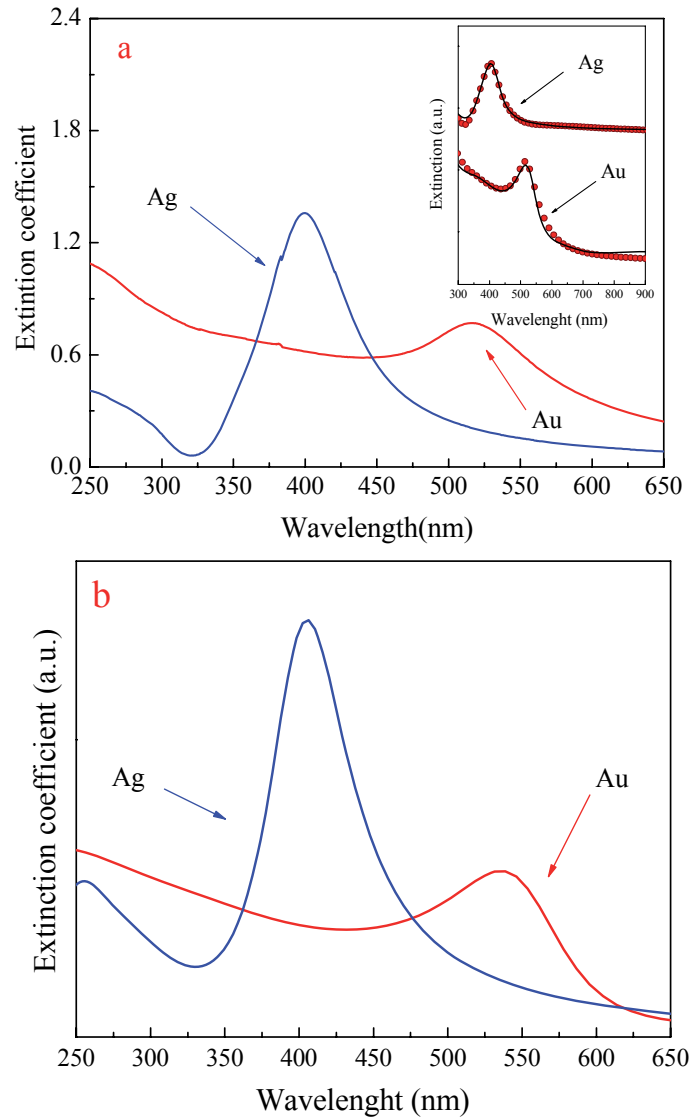
Fig. 3. – a) Surface Plasmonic Resonance spectra of silver and gold nanoparticles. The inset shows the best fit of experimental spectra (dot) with the Mie-Gans model we have adopted (continuous lines). b) Simulated PR spectra of silver and gold nanocolloids in water. The high-frequency features before maxima are due to interband transitions.

produces a continuous supply of ablated material in the plume; this is the source of the plasma intense luminosity. In fact, the vaporizing species are highly excited ionic particles, that incoherently relax towards fundamental quantum states emitting electro-magnetic radiations. The emission process is however different from that occurring in a LASER resonator, since the light emission from the plume is spontaneous and it is not coherently stimulated as in the laser effect. As shown in fig. 2, the plasma appears strongly illuminated due to these incoherent emission processes.
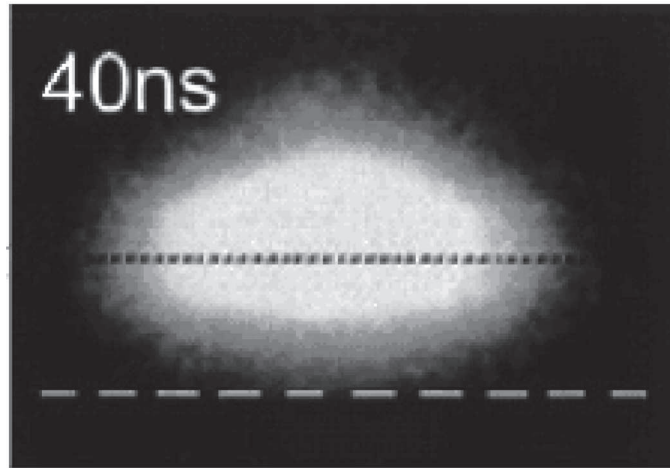
Fig. 4. – Image (taken from ref. [13]) of the expansion volume of the plasma plume in the graphite ablation in water, with laser pulses having 40 ns pulse duration.

Thermodynamic and kinetic factors may influence the formation of different phases due to the evolution of the laser-induced plasma. As reported by Yang [13], three are the thermodynamic factors which are of importance in determining the nature of phases in the plasma. These are: density of ablated species, temperature and pressure in the plasma.

The first parameter, *i.e.* the density of ablated species, may be evaluated by measurements of the expansion volume of the plasma plume itself. In practice, this expansion volume and the amount of the ablated species here contained, is measured through the volume of the hole which remains on the target surface after the ablation.

As shown in fig. 4, taken from Yang's review [13], the expansion volume of the plasma is measured through the images of the light emitting region on the surface. In this case the image refers to a graphite target submerged in water [14]. In such an experiment, the volume of the plasma plume, being a hemisphere of diameter corresponding to the FWHM intensity of emitted light, is estimated as $9.9 \times 10^{-7} \, \mathrm{cm^3}$. Assuming that the hole volume on the surface of target is linearly increased by the number of pulses, the ablation volume for a single pulse is determined to be $7.4 \times 10^{-8} \, \mathrm{cm^3}$. Therefore, the density in the plasma plume of carbon species, coming from graphite ablated with pulses of a Nd:YAG laser, resulted $6.7 \times 10^{21} \, \mathrm{cm^{-3}}$.

The second thermodynamic parameter is the extra temperature of the plasma plume. This is measured, as in a pirometer, through the optical emission spectra of the ablated species from the plasma confined in the liquid medium. Again, using a graphite target as ablation source, a plume temperature of ca. 5000 K has been determined when the optical emission spectra of C_2 molecules are measured. These species were obtained in water, ablating the target with a Nd:YAG laser at 1064 nm, and pulses having 20 ns duration and energy fluence of $10 \, \mathrm{J/cm^2}$ [14].

Finally we must talk of the third parameter, *i.e.* the pressure. By conducting in the liquid state the ablation of a solid target with a pulsed laser, this parameter depends on the sum of two contributions. The first one is the adiabatic expansion of the plasma under the confinement action of the liquid. In this medium an acoustic wave propagates
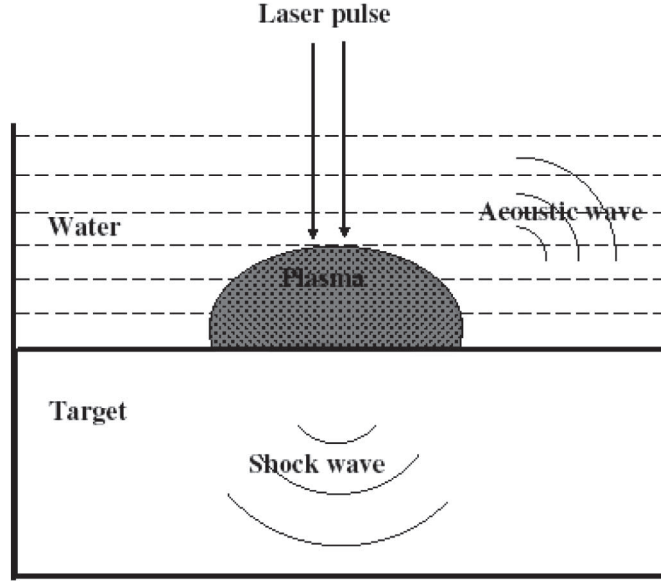
Fig. 5. – A scheme (taken from ref. [13]) showing the acoustic waves propagation in the confining liquid (water), and the shock waves generation inside the solid target.

longitudinally under the action of the expanding plasma, whilst a shock wave will propagate in the bulk of the solid target. Such situation is schematically depicted in fig. 5, taken from ref. [13]. Thus, the shock wave inside the solid target is the origin of the second contribution to the extra pressure generated in the system, when the plume is obtained for ablation in a liquid. Many experimental techniques have been developed, especially by Fabbro and co-workers [15-20], to measure the pressure generated by the shock wave propagating inside the solid target. These experiments were also accompanied by the development of theoretical models for the extra pressure due to the shock waves, done by the same author and his school.

The shock waves induce in the plasma plume extra conditions of pressure, temperature and density. As to the pressure increase, for instance, Berthe [19] reported a pressure of 2–2.5 GPa, when pulses of 50 ns from the wavelength $0.308\,\mu\text{m}$ of a XeCl excimer laser were employed. With shorter pulse durations, as for instance 3 ns, pressures up to 10 Gpa have been reported. Concerning density and temperature values, densities up to 10^{22}–10^{23} atoms/cm^3 have been reported for the ablated species in the plasma, and the plume temperature reaches values of 4000–5000 K [14].

From Fabbro's studies [15-20], a relationship for the extra pressure in the plasma can be given as

$$(3.1) \qquad P(\text{GPa}) = 0.01\sqrt{\frac{\alpha}{\alpha+3}}\sqrt{Z(\text{gcm}^{-2}\,\text{s}^{-1})\sqrt{I_0(\text{GWcm}^{-2})}},$$

α being the internal energy fraction which is of thermal nature ($\alpha \approx 0.25$), I_0 the intensity of incident power, and Z the reduced shock impedance between the confining liquid medium and the solid target. In the case of water as liquid medium, Z is defined

by the formula

$$2/Z = 1/Z_{\text{water}} + 1/Z_{\text{target}}. \tag{3.2}$$

To give an example of the Z values [15-20], for aluminum and silicon targets, ablated in water as submerging medium, these are: $Z_{\text{water}} = 0.165 \times 10^6$, $Z_{\text{aluminum}} = 1.5 \times 10^6$, and $Z_{\text{silicon}} = 2.1 \times 10^6$, the units being $\text{g cm}^{-2}\,\text{s}^{-1}$. In our case, the corresponding values have been measured to be $Z_{\text{gold}} = 1.96 \times 10^6$ and $Z_{\text{silver}} = 1.33 \times 10^6 \,\text{g cm}^{-2}\,\text{s}^{-1}$, respectively. With these values of Z, and assuming for α the value 0.25, pressures in the range 2.8–5.2 Gpa were obtained as a function of our I_0 values. It must be noted that the plasma state is very far from the thermodynamic equilibrium, so that the application of any type of state equation to evaluate the real pressure from the temperature value is not possible. For instance, if one assumed the plasma state as an ideal gas in thermodynamic equilibrium and applied the relevant state equation $P = nN_aK_BT/V$, N_a and K_B being the Avogadro and Boltzmann constants, respectively, the estimated pressure by such equation would result much lower than that measured in the plasma plume in experiments of pulsed laser ablation in liquids.

Under equilibrium conditions, the propagation velocity may be expressed with the formula

$$c = \sqrt{\left(\frac{\partial p}{\partial \rho}\right)_S} = \sqrt{\gamma \left(\frac{\partial p}{\partial \rho}\right)_T}. \tag{3.3}$$

The quantity c is a thermodynamic property of the system and constitutes the speed of propagation of the sound waves. In the perfect gas approximation, $c = \sqrt{\gamma \frac{p}{\rho}} = \sqrt{\gamma kT/m}$ being $\gamma = C_p/C_v = 1 + R/C_v$. The linearised equation of motion becomes

$$\frac{\partial v}{\partial t} + \frac{c^2}{\rho_0}\frac{\partial \rho}{\partial r} = 0. \tag{3.4}$$

Introducing the continuity equation, where the term $(v \cdot \frac{\partial \rho}{\partial r})$ is a very small quantity of the second order, we get the *linearized equation of continuity* in the form [21]

$$\frac{\partial \rho}{\partial t} + \rho_0 \left(\frac{\partial}{\partial r} \cdot v\right) = 0. \tag{3.5}$$

Regarding the kinetic aspects, there are some peculiarities of PLA in liquid confined targets. Surprisingly, the velocity of ablation of a solid target submerged in a liquid medium is much higher than the corresponding velocity in vacuum or in a diluted inert gas. In fact, due to the confining action operated by the submerging liquid, the plasma having the above said characteristics of high temperature, pressure, and density, can continuously etch the solid target at the interface solid-plasma, not expanding very far from the etched target as happens in the vacuum, or in diluted gas environments [13]. In fig. 6 we show the effects of laser ablation of a silicon target with an UV laser, having pulses in the range of 20–30 ns, when two different confining media, *i.e.* water and air, are submerging the target [22-25]. It is also shown as the thickness of the submerging water has a maximum efficiency at a definite depth, but it decays more than linearly when the
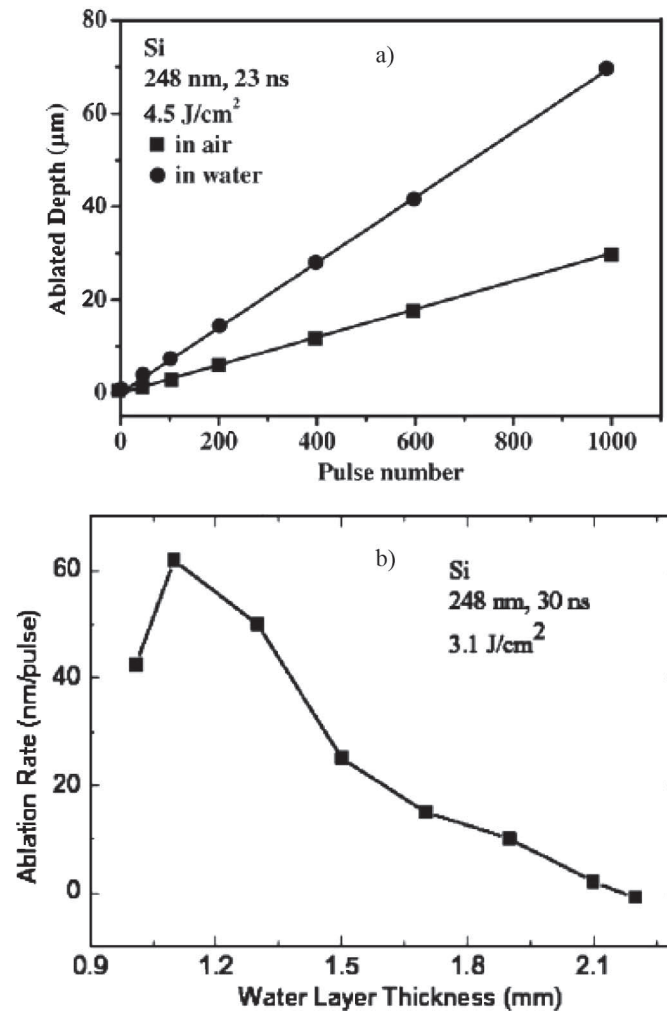
Fig. 6. – The effects, on the ablated particle amounts, of different confining media (a) and of the layer thickness (b) in PLAL experiments (taken from ref. [13]).

thickness of submerging layer overcomes a certain value. Although the layer thickness of the submerging liquid is very important for the mechanisms of energy dissipation, the maximum observed at a certain value of thickness in the plot ablation rate *vs.* layer thickness (fig. 6b) may be explained with the minor possibility given to the plasma plume to expand when the layer of the submerging medium is less. Therefore, a more confined plasma, around the etched point in the target, will concentrate better the energy due to the high temperature and high pressure of the plume, to promote more easy etching of the solid sample.

The mechanism seems to be controlled by the shock waves generated in the target under the laser pulses having an opportune fluency, because they decay into acoustic mechanical waves in the liquid medium that are called *ablative piston*. The action exerted by the *ablative piston* enhances that one due to extra pressure and high temperature of the plume increasing the ablation rate.
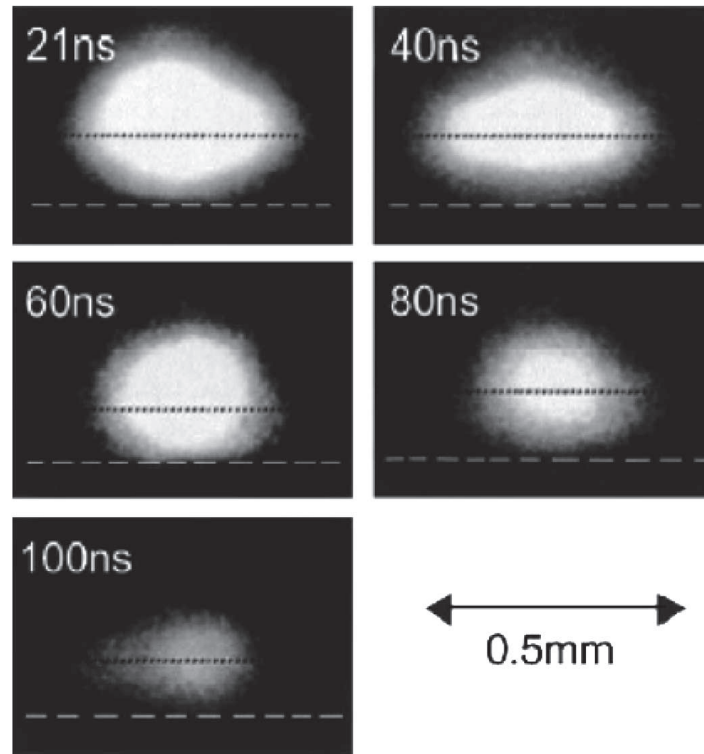
Fig. 7. – Influence, on the expansion volume of the plasma plume, of the laser pulses duration (taken from ref. [13]).

Because the confining liquid absorbs the laser energy in the beam crossed layer [6], the etching action by the plasma plume and the depth of the liquid layer must reach a right compromise. The absorption of the laser beam energy by the submerging liquid produces so high temperature increase in the crossed layer, that the density of heated portion of liquid may be strongly modified respect to the equilibrium value [1], especially if the density *vs.* temperature curve of the relevant submerging liquid has a great slope. On the other side, the depth of the liquid layer can reduce the ablation threshold of the solid target by the action of two concurring effects: the confinement of the plasma near to the target surface and the dissipation of the plasma temperature at the plasma-liquid interface. In conclusion, high production of ablated particles by PLA in confining liquid media is possible either for thin films deposition or for small particles synthesis [13].

An important kinetic aspect of PLA in liquid media is the rapid dissipation of the plasma plume energy at the boundary of the confining liquid. Such a quenching action determines, from one side, the possibility to repetitive shoot on the surface target by the pulsed laser beam and this fact increases the amount of produced ablated species, but, from another side, determines the heating of the layer strictly in contact with the plume and crossed by the laser beam; we noticed that this fact affects the density variations of such layer [6]. The rapid quenching action operated by the presence of liquid medium can be seen in fig. 7, taken from ref. [13]. Here the plasma light emission in water, of a solid graphite target is generated in PLAL experiments with different pulse duration.
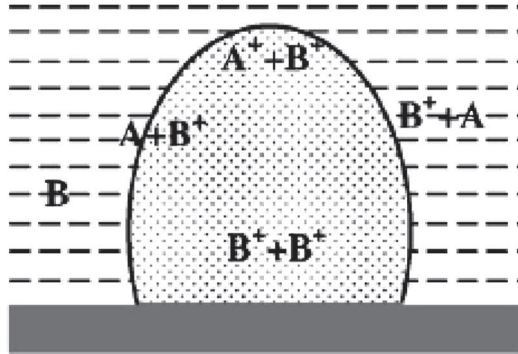
Fig. 8. – A scheme (taken from ref. [13]) showing the chemical reactions occurring between solute (A), solvent (B) and among their ions, inside the plasma plume and at the plume-solvent interface.

One can see, from the dimensions of emitting plume volume, that with longer duration of pulses, the confining action of the liquid in dissipating the energy of system is more efficient.

In fact, in the case of liquid confined plasma, the plume is confined near to the target surface, thus providing a continuous supplying of ablated material which, in state of plasma, enforces the luminosity of the emission [13].

Finally, the cooling effect operated by the liquid confining medium should enhance the formation in the plasma plume of metastable structures and phases. These rapidly convert to the stable phases due to the short quenching times that the confining liquid exerts at the plasma-liquid interface. These metastable phases are the results of the reactions occurring inside the plasma and at the plasma-liquid interface due to the high temperature and high pressure conditions. In fig. 8, taken by ref. [13], a series of chemical reactions between B (solvent) and A (solid target), and among their ions, are schematically reported. Of course, changing either A or B, these reactions will strongly change, also because the possibility of having ionic species in the plume and at the interface depends on the ionisation energies of the relevant species. In our laboratory, it has been shown that the nature of ablated species coming from the same target will change in different liquid media [26]. The plasmonic resonance spectra (see following paragraph), have been used to reveal these differences, depending on the used solvent.

Of course, a compressed treatment like this, does not allow to speak of many other physical aspects that are important in plasma states. These are, for instance, the role played by the discontinuities in the distribution function of plasma electrons, and as these discontinuities can be modelled with approaches deriving from the continua mechanics. Moreover, it should be important to introduce the effect of the electric fields inside the plasma due to the plasma electrons and to the ions, on the mechanical waves propagating in the plasma plume. The effect is in practice a wave-breaking one, when the intensity of the electric field inside the plasma plume overcomes certain critical values.

Shifting again our attention on the shock waves, we want to describe the hydrodynamic processes accompanying the waves' propagation [21].

First of all, we will define a shock wave a system in which the properties of a fluid phase change sharply within a very short distance in the space. There is in the gas phase, a certain tendency of any compression-wave to transform into a shock wave. Neglecting in the hydrodynamic equations terms involving thermal conductivity, diffusion, and

viscosity, the shock wave manifests itself as a mathematical discontinuity in the solutions. However, including these dissipative terms, the effect is that to change the discontinuity in a transition slightly more gradual, which for instance, in a gas at TPS conditions, occurs within a distance of few mean free paths, *i.e.* approximately within 10^{-5} cm [21]. Due to such sharp gradients in the macroscopic properties of a gas subjected to a shock wave, the Navier-Stokes equations are not sufficiently accurate to describe both structure and thickness of the wave. We tried to apply at our system of plasma plume the *Hugoniot equations* for a steady-state one-dimensional problem [7,8]. Assuming that the derivatives at $x = -\infty$ are zero, we obtain the relations below between the variables in the two sides of the shock wave:

$$(3.6) \qquad\qquad M = \rho_0 v_0 = \rho_\infty v_\infty,$$

$$(3.7) \qquad\qquad M v_0 + p_0 = M v_\infty + p_\infty,$$

$$(3.8) \qquad\qquad H_0 + (1/2){v_0}^2 = H_\infty + (1/2){v_\infty}^2.$$

These relations, called the *Hugoniot relations*, correlate the eight quantities ρ_0, v_0, p_0, H_0, ρ_∞, v_∞, p_∞ and H_∞. However, using the thermodynamic dependence of H on ρ and p, the number of variable is reduced to six [21]. Thus, the equations are sufficient to express three of the variables in terms of the remaining three. Usually, we will specify the density and pressure on the low pressure side of the shock wave, ρ_0 and p_0, together with an additional parameter which indicates the strength of shock, for instance the pressure on the high side, p_∞. The equations are then solved to obtain the values of the remaining quantities v_0, v_∞, and ρ_∞. The v_0 value represents the velocity of propagation of the shock wave into the expanding plasma, on the low pressure side. v_∞ is instead the velocity of hot gases away from the wave front of the plasma.

We rearranged the *Hugoniot equations* in a different form, and from the equations of continuity and motion (eqs. (3.6) and (3.7)) we obtained

$$(3.9) \qquad\qquad M = \left(\rho_0 \rho_\infty \frac{p_\infty - p_0}{\rho_\infty - \rho_0} \right)^{1/2}.$$

Moreover, because $1/2({v_\infty}^2 - {v_0}^2) = 1/2(v_\infty - v_0)(v_\infty + v_0)$, using the same couple of equations, we may obtain [21]

$$(3.10) \qquad\qquad 1/2({v_\infty}^2 - {v_0}^2) = -\frac{(p_\infty - p_0)(\rho_\infty + \rho_0)}{2\rho_\infty \rho_0}.$$

Now, combining this result with the conservation of energy equation, (3.8), and using the relation $H = U + p/\rho$ we have got the relation

$$(3.11) \qquad\qquad (U_\infty - U_0) = \frac{(p_\infty + p_0)(\rho_\infty - \rho_0)}{2\rho_0 \rho_\infty}.$$

Equations from (3.9) to (3.11) can be considered the *Hugoniot equations* in a more convenient form.

As we cannot solve explicitly these equations, we have introduced the equation of state and the thermodynamic conditions for the gas in the plasma plume. These are of

course large but necessary approximations, and allowed us to calculate values of pressure in the plasma going from ca. 2.8 GPa to ca. 5.2 Gpa, depending on the laser energy we released over the target, whilst the temperature was estimated by the plume luminosity to be around 4200 K. With the same above equations and the *ideal gas* approximations, we obtained energy values of the order of 2.5 J in the plasma, values that are well above those of the impinging pulses of the laser. Therefore, the role played by the energetics of chemical reactions in the plume, and at confining liquid-plume interface, to enhance the energy well above the threshold given by the laser pulses is undoubtedly dominant.

3˙2. *The optical properties of noble metal nanoparticles*. – The optical properties of the PLAL produced nanocolloids regulate their absorption in the visible spectral region, the so-called Plasmonic Resonance (PR) spectra. On the other hand, these spectra also depend on the sizes and shapes of the relevant particles [27].

In our laboratory either SERS [2] and catalytic applications [28] have been carried out in these last years by the use of silver and gold nanoclusters. Especially in the latter case, an estimative measure of gold particle dimensions has been made by low-frequency Raman modes (LOFIS modes) and their behaviour under different polarization conditions of incident laser light [29]. It is well known in fact, since the pioneer work by Lamb [30], that surface acoustic phonons propagate in assumed spherical nanometric objects, producing dilatational and shear motions that scatter quasi elastically the visible light as a consequence of density fluctuations [31-33].

The Raman frequency shift, with respect to the elastic peak, is inversely correlated to the radius of the particle through the sound propagation speed and a dimensionless constant whose value is assumed to vary within a restricted range between 0.7 and 0.9, depending on the material [31-33]. Due to the acoustic nature of these features in the low-frequency Raman spectra of the nanoobjects, one can retrieve analogies with the hydrodynamic triplet of the Rayleigh-Brillouin spectra [34], where the Brillouin frequency shift is proportional to the sound propagation speed in the relevant medium through the transferred wave vector. On the other hand, in the equation describing the transferred wave vector, one has at the denominator the wavelength of the scattered light, which plays the role of length as that of the particle size in the LOFIS spectrum counterpart.

The visible absorption (PR) of these colloids is instead interpreted at the light of the Mie theory [35], introducing the Gans approximation [36], to take into account the role played by the dielectric function of liquid medium in which the colloids are suspended.

Therefore, our spectra have been modelled, in the framework of Mie's theory, with the equation given by Papavassiliou [37], for the extinction coefficient K defined for N particles of volume V.

$$(3.12) \qquad K = 4.5 \times 10^7 \, NV \, E\varepsilon_m{}^{3/2}\varepsilon_2/[(\varepsilon_1 + 2\varepsilon_m)^2 + \varepsilon_2{}^2].$$

In eq. (3.12) E is the photon energy in eV, V is the particle volume in m^3, ε_1 and ε_2 are the real and imaginary components of complex dielectric function. It is interesting to note that K has the dimensions of a cross-section (the quantity given in eq. (3.12) is in m^2), which can be directly considered for a valuation of the total amount of metallic atoms present in the sample, through the use of the atomic density. In this regard, we would like to stress that HR-TEM data are of relevant importance for a check of the sample shape or size. In fact, for particles smaller than the bulk electronic mean-free path, the dielectric function of the metal must be corrected for quantum size effects (QSE). This point must be considered with much attention, because it directly influences the

particles' optical response and may be taken into account if one considers a classic Drude model. In this case the dielectric function of each metallic cluster can be expressed as

$$(3.13) \qquad \varepsilon = \varepsilon_b(E) + 1 - E_p{}^2/(E^2 + i\lambda E).$$

In this equation λ, correlated with the experimental width of the Mie absorption, can be considered as a damping factor to make terms on the right-hand side of eq. (3.13) not vanish, excluding the $\varepsilon_b(E)$ term, when $E = E_p$, *i.e.* at resonance conditions. It measures also the mean collision rate of conduction electrons at optical frequencies. $\varepsilon_b(E)$ is the contribution coming from interband transitions and from all other non-conduction electrons to the dielectric function of the matal, E_p is the plasma energy of free electrons, *i.e.* the PR energy at the absorption maximum.

When the particles are not too small, one can correct the dielectric function approximately by modifying the λ value. For very small particles the QSE corrections can be complicated and may result in band narrowing, band splitting and frequency shifts in either directions from the PR band centre of bulk particles. The range of sizes for this correction on the PR spectra has been detailed in ref. [27], and this is the case in our experiments. The general expression which takes into account a classic QSE relatively to λ quantity is the following:

$$(3.14) \qquad \lambda = \lambda_B + A\nu_F/R.$$

Recently it has been shown [27,38,39] that it is possible to fit, by the use of very few fitting parameters, the PR spectra of gold colloids starting from the known bulk optical constants of the metal and correcting them for the above-mentioned QSEs.

Looking at fig. 3, it is possible to remark the very nice agreement obtained between the adopted model and our experiments. In the inset we show the best fit of the experimental PR spectra of both metals, obtained with the Mie-Gans model we have used. Figure 3b shows the simulated PR spectra of silver and gold, when the simulation was performed by taking into account the role of the complex dielectric function of the system constituted by water and the relevant metal colloids.

4. – Conclusions

The experiments that we are carrying out on the laser ablation of noble metal solid targets in liquid media present many aspects which involve the physics of the plasma plume and the chemical reactions occurring in this phase, under the non-equilibrium state whose conditions of high pressure, temperature and density are determining. These aspects have been treated in this paper, with a complete description of the theories which underlie the plasma behaviour. These have been described in the light of non-equilibrium fluid mechanics, applying the Hugoniot equations to the situations present in our experiments. Under the approximations that the problem requires for the solution of these equations, the values of extra pressure, extra temperature and energies of our system have been obtained.

A second aspect treated in this paper regards a description of the optical properties of the nanoparticles that are produced in our experiments. These are related to the surface plasmonic resonance spectra in the visible spectral region. When the PR spectra of these particles in water are modelled by means of the Mie-Gans theory, our spectra are nicely reproduced, taking into account the dependence of the PR maximum on the dielectric function of medium, and quantum size effects that we must introduce in the model for the nanometer-scale sizes of produced objects.

REFERENCES

[1] OGALE S. B., PATIL P. P., PHASE D. M., BHANDARKAR Y. V., KULKARNI S. K., KULKARNI SMITA, GHAISAS S. V., KANETKAR S. M., BHIDE V. G. and GHUA S., *Phys. Rev. B*, **36** (1987) 8237.
[2] COMPAGNINI G., PATANÈ G., D'URSO L., PUGLISI O., CATALIOTTI R. S. and PIGNATARO B., *J. Phys. Chem. C*, **112** (2008) 20301.
[3] BRYANT M. A. and PEMBERTON J. E., *J. Am. Chem. Soc.*, **113** (1991) 3629.
[4] KUDELSKI A. and KRYSINSKI P., *J. Electroanal. Chem.*, **443** (1998) 5.
[5] SHEN A. and PEMBERTON J. E., *Phys. Chem. Chem. Phys.*, **1** (1999) 5677.
[6] COMPAGNINI G., MESSINA E., CATALIOTTI R. S., GRILLO A. and GIAQUINTA G., *Philos. Mag. Lett.*, **89** (2009) 250.
[7] COURANT R. and FRIEDRICHS K. O., *Supersonic Flows and Shock Waves* (Interscience Press) 1948.
[8] COLE R. H., *Underwater Explosions* (Princeton University Press) 1948.
[9] COMPAGNINI G., MESSINA E., PUGLISI O., CATALIOTTI R. S. and NICOLOSI V., *Chem. Phys. Lett.*, **457** (2008) 386.
[10] FABBRO R., FOURNTIER J., BALLARD P., DEVAUX D. and VIRMONT J., *J. Appl. Phys.*, **68** (1990) 775.
[11] BERTHE L., FABBRO R., PEYER P., COLLIER L. and BARTNICKI E., *J. Appl. Phys.*, **82** (1997) 2826.
[12] FABBRO R., PEYER P., BERTE L. and SCHERPEREEL X. J., *Laser Appl.*, **10** (1998) 265.
[13] YANG G. W., *Prog. Mat. Sci.*, **52** (2007) 648.
[14] SAKKA T., TAKATANI K., OGATE Y. H. and MABUCHI M., *J. Phys. D: Appl. Phys.*, **35** (2002) 65.
[15] DEVAUX D., FABBRO R., TOLLIER L. and BARTNICKI E., *J. Appl. Phys.*, **74** (1993) 2268.
[16] PEYER P. and FABBRO R., *Opt. Quantum Electron.*, **27** (1995) 1213.
[17] PEYER P., SCHERPEREEL X. and FABBRO R., *J. Mat. Sci.*, **33** (1998) 1421.
[18] BERTHE L., FABBRO R., PEYER P. and BARTNICKI E., *J. Appl. Phys.*, **85** (1999) 7552.
[19] BERTHE L., SOLLIER A., FABBRO R., PEYER P. and BARTNICKI E., *J. Phys. D: Appl. Phys.*, **33** (2000) 2142.
[20] PEYER P., BERTHE L., FABBRO R. and SOLLIER A., *J. Phys. D: Appl. Phys.*, **30** (2000) 498.
[21] HIRSCHFELDER J. O., CURTIS C. F. and BIRD R. B., *Molecular Theory of Gases and Liquids* (J. Wiley & Sons, New York) 1967.
[22] GEIGER M., BECKER W., REBHAN T., HUTFLESS J. and LUTZ N., *Appl. Surf. Sci.*, **96-98** (1996) 309.
[23] ZHU S., LU Y. F., HONG M. H. and CHEN X. J., *J. Appl. Phys.*, **89** (2001) 2400.
[24] ZHU S., LU Y. F. and HONG M. H., *Appl. Phys. Lett.*, **79** (2001) 1396.
[25] KIM D. S., OH B. and LEE H., *Appl. Surf. Sci.*, **222** (2004) 138.
[26] SCALISI A. A., COMPAGNINI G. and PUGLISI O., *J. Appl. Phys.*, **94** (2003) 7874.
[27] LINK S. and EL-SAYED M. A., *J. Phys. Chem. B*, **103** (1999) 8410.
[28] CATALIOTTI R. S., COMPAGNINI G., CRISAFULLI C., MINICÒ S., PIGNATARO B., SASSI P. and SCIRÈ S., *Surf. Sci.*, **494** (2001) 75.
[29] CATALIOTTI R. S., COMPAGNINI G., MORRESI A., OMBELLI M. and SASSI P., *Phys. Chem. Chem. Phys.*, **4** (2002) 2774.
[30] LAMB H., *Proc. London Math. Soc.*, **13** (1882) 189.
[31] DUVAL E., BOUKENTER A. and CHAMPAGNON B., *Phys. Rev. Lett.*, **56** (1986) 2052.
[32] MONTAGNA M. and DUSI R., *Phys. Rev. B*, **52** (1995) 10080.
[33] FUJII M., NAGAREDA T., HAYASHI S. and YAMAMOTO K., *Phys. Rev. B*, **44** (1991) 6243.
[34] BERNE B. J. and PECORA R., *Dynamic Light Scattering* (J. Wiley & Sons, Inc., New York) 1976.
[35] MIE G., *Ann. Phys.*, **25** (1908) 377.
[36] COMPAGNINI G., MESSINA E., PUGLISI O. and NICOLOSI V., *Appl. Surf. Sci.*, **254** (2007) 1007.

[37] PAPAVASSILIOU G. C., *Prog. Solid State Chem.*, **12** (1980) 185.
[38] AMENDOLA V., POLIZZI S. and MENEGHETTI M., *J. Phys. Chem. B*, **110** (2006) 7232.
[39] LINK S., WANG Z. L. and EL-SAYED M. A., *J. Phys. Chem. B*, **103** (1999) 3529.